ELSEVIER

Journal of Organometallic Chemistry 512 (1996) 165–173

Journal of Organometallic Chemistry

Effects of steric strain on the bonding in zinc metallocenes: the structure of $[(C_3H_7)_4C_5H]_2Zn$

David J. Burkey, Timothy P. Hanusa *

Department of Chemistry, Vanderbilt University, Nashville, TN 37235, USA

Received 5 July 1995; in revised form 18 September 1995

Abstract

Zinc diiodide reacts with the potassium salts of 1,2,4-tri- and 1,2,3,4-tetra(isopropyl)cyclopentadiene to form the corresponding zinc metallocenes in high yield. Both compounds are highly air-sensitive, but $[(C_3H_7)_4C_5H]_2Zn$ is isolated as a high-melting crystalline solid, whereas $[(C_3H_7)_3C_5H_2]_2Zn$ is a waxy solid that melts just above room temperature. Like other structurally characterized zincocenes, $[(C_3H_7)_4C_5H]_2Zn$ has an asymmetric "slipped-sandwich" structure with one η^1- and one approximately η^5-ring. The Zn–C distance for the η^1-ring of 2.223(4) Å is the longest yet observed in a zincocene. The Zn–C distances for the η^5-ring cover a larger than usual range (0.52 Å), and include the shortest Zn–C ring bond reported in a cyclopentadienyl zinc complex (1.991(4) Å). These extremes in structural values reflect the increased slippage of the rings in $[(C_3H_7)_4C_5H]_2Zn$, which is a consequence of the exceptional steric bulk of the $[(C_3H_7)_4C_5H]^-$ anion. Variable temperature NMR data for $[(C_3H_7)_4C_5H]_2Zn$ are consistent with the existence of an asymmetric structure in solution.

Keywords: Zinc; Metallocene; Cyclopentadienes; Slipped-sandwich; Fluxional behavior

1. Introduction

The highly asymmetric structures of beryllocene (Cp_2Be) and the zincocenes (Cp'_2Zn) have proven difficult to characterize unambiguously. When Cp_2Be was first synthesized in 1959 by Fischer and Hofmann [1], it was found to possess a permanent dipole moment in solution, which ruled out a symmetrical sandwich geometry for the complex analogous to that of ferrocene (Fig. 1). An initial gas phase electron diffraction study of Cp_2Be identified an unsymmetrical sandwich geometry for the complex [2,3], while several molecular orbital calculations favored an asymmetric π, σ-structure [4–7], with an ionically bound η^5-Cp ring and a covalently bound η^1-Cp ring. A low temperature single crystal X-ray investigation of Cp_2Be revealed that the complex possesses a "slipped-sandwich" structure in the solid state [8]; subsequent experiments confirmed that this is likely to be the ground state geometry for the complex in solution as well as in the gas phase [9–11]. A gas phase electron diffraction study of Cp^*_2Zn [12,13], and an X-ray study of $(Me_4PhC_5)_2Zn$ [14], revealed that these monomeric zinc metallocenes also possess slipped-sandwich geometries similar to that of Cp_2Be.

Why do beryllocene and zincocenes not form symmetrical sandwich structures? A generally accepted explanation is that the metal–carbon bond strength for Be and Zn is not enough to cause complete localization of the cyclopentadienyl anion. Enough covalency exists in the M–C interaction, however, that a symmetric, completely ionic structure ($[Cp']^-[M]^{2+}[Cp']^-$) is also disfavored. Therefore, neither contribution to the total energy dominates, and one ring interacts so that its coordination is intermediate between fully ionic (i.e. pentahapto) and fully-covalent (monohapto); this type of bonding interaction has been termed "peripheral" [11].

Although there is reasonable consensus about the forces that contribute to the slipped-sandwich geometries of beryllocene and zinc metallocenes, how much ionicity or covalency exists in the bonding between the metal and the cyclopentadienyl rings is still controversial. We have been using the 1,2,4-tri- and 1,2,3,4-tetra(isopropyl)cyclopentadienyl ligands ($[Cp^{3i}]^-$ and

* Corresponding author.

SSDI 0022-328X(95)05952-0

$[Cp^{4i}]^-$ respectively) to explore the effects that extremely bulky rings have on the properties and structures of main-group metallocenes [15–17]. In the $(Cp^{4i})_2M$ (M = Mg–Ba, Sn) complexes, the metal is effectively encapsulated; e.g. the compounds do not react with nucleophiles and often display enhanced air-stability compared with metallocenes having less encumbering cyclopentadienyl ligands. Although only a single isopropyl group is removed from each ring in the $(Cp^{3i})_2M$ metallocenes, the resistance to adduct formation with Lewis bases, and the improved air-stability of the $(Cp^{4i})_2M$ complexes, vanish. Investigation of zinc metallocenes containing $[Cp^{3i}]^-$ and $[Cp^{4i}]^-$ ligands thus provides an opportunity to determine whether a different metallocene geometry will either reduce or increase the differences caused by the two ligands. The synthesis of $(Cp^{4i})_2Zn$ also allows us to study how the presence of the extremely bulky $[Cp^{4i}]^-$ ligand affects the unusual bonding found in zinc metallocenes.

2. Experimental details

2.1. General considerations

All manipulations were conducted with the rigid exclusion of air and moisture using high vacuum, Schlenk, or drybox techniques. Proton and carbon (^{13}C) NMR spectra were obtained on a Bruker NR-300 spectrometer at 300 MHz and 75.5 MHz respectively, and were referenced to the residual proton and ^{13}C resonances of C_6D_6 (δ 7.15 and 128.0). Assignments in the ^{13}C NMR spectra were made with the help of DEPT pulse experiments. Variable temperature NMR experiments were recorded on a Bruker NR-400 spectrometer at 400 (^1H) and 100.6 (^{13}C) MHz, and were referenced to the residual methyl resonances of toluene-d_8 (δ 2.09 and 20.4). Temperatures in the VT-NMR experiments were calibrated with CH_3OH [18]. Infrared data were obtained on a Perkin-Elmer 1600 series FT-IR spec-

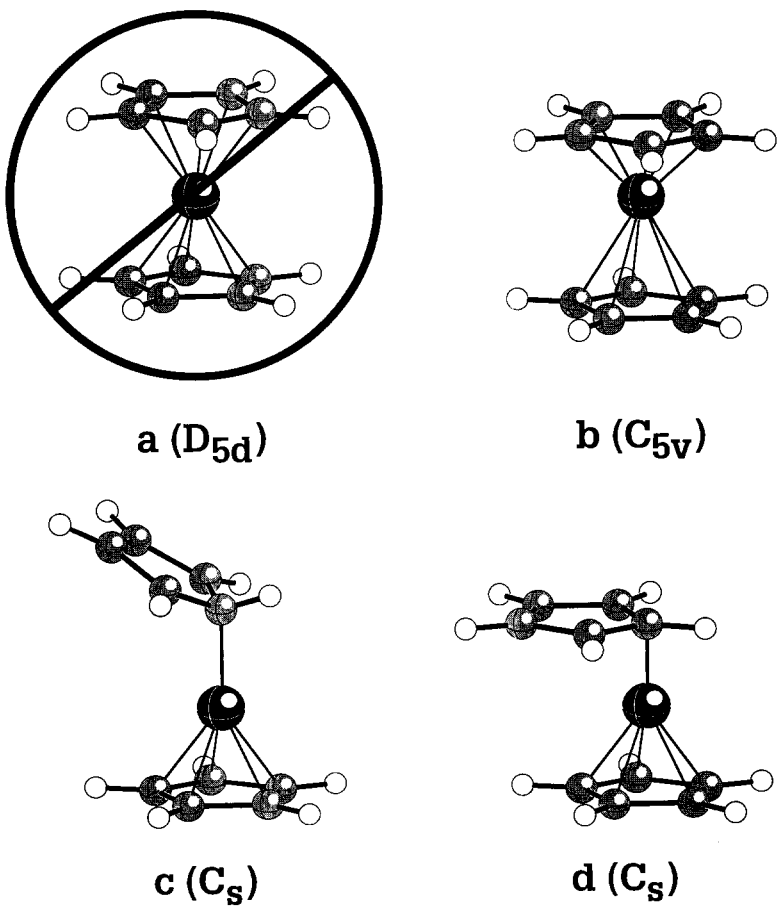

Fig. 1. Progression of proposed structures for beryllocene: (a) a symmetrical ferrocene-like structure was ruled out based on dipole moment measurements [1]; (b) an unsymmetrical sandwich geometry deduced from early electron diffraction measurements [2,3]; (c) an asymmetric π, σ-structure favored by some theoretical studies [4–7]; (d) the "slipped sandwich" geometry found by low-temperature X-ray diffraction [8].

trometer. KBr pellets for IR spectroscopy were prepared as previously described [15]. Elemental analyses were performed by Oneida Research Services, Whitesboro, NY.

2.2. Materials

KCp^{3i} ($[Cp^{3i}]^- = 1,2,4\text{-}(C_3H_7)_3C_5H_2$) and KCp^{4i} ($[^iCp^{4i}]^- = 1,2,3,4\text{-}(C_3H_7)_4C_5H$) were prepared using literature procedures [15]; they were isomerically pure by ^1H NMR (THF-d_8). ZnI_2 was a commercial sample (Aldrich) and was used as-received. Anhydrous diethyl ether was purchased from Aldrich and stored over 4A molecular sieves before use; all other solvents for reactions were distilled under nitrogen from sodium or potassium benzophenone ketyl. NMR solvents were vacuum distilled from Na/K (22:78) alloy and stored over 4A molecular sieves.

2.3. Synthesis of $(Cp^{3i})_2Zn$

In a glovebox, KCp^{3i} (1.11 g, 4.81 mmol) and ZnI_2 (0.74 g, 2.32 mmol) were added to 35 ml of Et_2O in an Erlenmeyer flask; the yellow suspension was then stirred for 12 h. The ether was removed under vacuum and the residue was extracted with 50 ml of hexanes. Subsequent filtration of the reaction mixture and removal of the hexanes under vacuum from the filtrate gave 0.95 g (91% yield) of $(Cp^{3i})_2Zn$ as a pale yellow oil. On long standing under ambient conditions (1–2 months), samples of $(Cp^{3i})_2Zn$ partially solidified into a soft, waxy solid (m.p. ca. 30°C). Anal. Found: C, 75.43; H, 10.52. $C_{28}H_{46}Zn$. Calc.: C, 75.06; H, 10.35. ^1H NMR (C_6D_6): δ 5.47 (s, 4 H, ring–C*H*); 2.88 (septet, $J = 6.9$ Hz, 2 H, C*H*Me_2); 2.73 (septet, $J = 6.8$ Hz, 4 H, C*H*Me_2); 1.24 (d, $J = 6.9$ Hz, 12 H, CH_3); 1.19 (d, $J = 6.6$ Hz, 12 H, CH_3); 1.17 (d, $J = 6.8$ Hz, 12 H, CH_3). ^{13}C NMR (C_6D_6): δ 134.2 (ring–*C*CHMe$_2$); 130.8 (ring–*C*CHMe$_2$); 91.1 (ring–*C*H); 29.0 (*C*HMe$_2$); 26.8 (*C*HMe$_2$); 25.7 (*C*H$_3$); 24.5 (*C*H$_3$); 24.3 (*C*H$_3$). Principal IR bands (neat, cm^{-1}): 2961 (s), 1460 (s), 1381 (s), 1362 (s), 1324 (w), 1304 (w), 1280 (w), 1262 (w), 1224 (w), 1176 (m), 1103 (m), 1030 (s, br), 959 (w), 918 (w), 864 (m, sh), 813 (s), 678 (w), 487 (w).

2.4. Synthesis of $(Cp^{4i})_2Zn$

In a glovebox, an Erlenmeyer flask was charged with KCp^{4i} (0.49 g, 1.79 mmol) and ZnI_2 (0.28 g, 0.89 mmol); Et_2O (25 ml) was then added and the yellow suspension was stirred for 12 h. The Et_2O was removed under vacuum; the residue was extracted with 30 ml of hexanes and filtered through a glass frit. The hexanes were subsequently removed from the filtrate to give a waxy residue; fractional sublimation of this solid (100–140°C, 10^{-6} Torr) gave 0.38 g of $(Cp^{4i})_2Zn$ (80% yield) as an ivory–white powder (m.p. 123–125°C). Anal. Found: C, 76.51; H, 11.32. $C_{34}H_{58}Zn$. Calc.: C, 76.73; H, 10.98. ^1H NMR (C_6D_6): δ 5.43 (s, 2 H, ring–C*H*); 3.09 (septet, $J = 7.2$ Hz, 4 H, C*H*Me_2); 2.89 (septet, $J = 6.8$ Hz, 4 H, C*H*Me_2); 1.31–1.35 (two overlapping doublets, 24 H, CH_3); 1.22 (d, $J = 6.8$ Hz, 12 H, CH_3); 1.04 (d, $J = 6.6$ Hz, 12 H, CH_3). ^{13}C NMR (C_6D_6): δ 131.3 (ring–*C*CHMe$_2$); 122.3 (br, ring–*C*CHMe$_2$); 93.7 (ring–*C*H); 27.7 (*C*HMe$_2$); 27.2 (*C*HMe$_2$); 26.2 (*C*H$_3$); 24.6 (*C*H$_3$); 24.2 (*C*H$_3$); 24.1 (*C*H$_3$). Principal IR bands (KBr, cm^{-1}): 2861 (s, br), 1457 (s), 1379 (s), 1362 (s), 1308 (m), 1262 (w), 1221 (w), 1174 (m), 1130 (m), 1106 (m), 1065 (m), 972 (m), 902 (m), 880 (w), 784 (s), 712 (w), 613 (w), 538 (w), 492 (m). Crystals of $(Cp^{4i})_2Zn$ suitable for X-ray diffraction were grown by slow evaporation of a saturated THF solution at room temperature.

Table 1
Crystal data and summary of data collection for $[(C_3H_7)_4C_5H]_2Zn$

Formula	$C_{34}H_{58}Zn$
Formula weight	532.21
Crystal color	colorless
Crystal dimensions (mm^3)	0.36×0.48×0.90
Space group	$P\bar{1}$
Cell dimensions (20°C)	
a (Å)	9.583(1)
b (Å)	11.4982(8)
c (Å)	8.5913(6)
α (°)	107.613(6)
β (°)	97.049(8)
γ (°)	112.896(6)
Volume (Å^3)	799.4(1)
Z	1
Calculated density (g cm^{-3})	1.105
Absorption coefficient (cm^{-1})	11.71
Type of scan	ω–2θ
Scan speed (° min^{-1})	8.0
Scan width	1.68 + 0.3 tan θ
Limits of data collection	$6° \leq 2\theta \leq 120°$
Total reflections	2553
Unique reflections	2388
Number with $I > 3.0\sigma(I)$	1773
R(F)	0.044
R_w(F)	0.064
Goodness of fit	2.45
max. Δ/σ in final cycle	0.01
Max./min. peak in final difference map (eÅ^{-3})	0.26/−0.29

2.5. X-ray crystallography of $(Cp^{4i})_2Zn$

A suitable crystal of the compound was sealed in a glass capillary tube. All measurements were performed on a Rigaku AFC6S diffractometer at 20°C with graphite monochromated Cu Kα radiation ($\lambda = 1.54178$ Å).

Relevant crystal and data collection parameters are given in Table 1.

Cell constants and orientation matrices for data collection were obtained from a systematic search of a limited hemisphere of reciprocal space; sets of diffraction maxima corresponding to a triclinic cell were located, whose setting angles were refined by least-squares. The space group was initially assumed to be $P\bar{1}$ from consideration of unit cell parameters and a statistical analysis of intensity distribution. Subsequent solution and refinement of the structure eventually confirmed this choice.

Data collection was performed using continuous ω–2θ scans with stationary backgrounds (peak/background counting time 2:1). Data were reduced to a unique set of intensities and associated sigma values in the usual manner. No decay was evident in the intensities of three representative reflections measured after every 150 reflections; psi scans of several intense reflections indicated that no correction for absorption was necessary. Considering that $Z = 1$ for the unit cell, the zinc atom was initially placed on an inversion center at (0.5, 0.5, 0.5); attempts to expand the structure from this point, however, were unsuccessful. Removing the constraints on the zinc revealed two different sites for it near the inversion center, each at half occupancy. The identification of most of the structure by direct methods (SIR) was then possible, although least-squares refinement of this partial solution converged with unreasonably high residuals (R(F) > 40%). An attempt was then made to solve the structure in the lower symmetry space group $P1$, which successfully revealed the entire structure. However, refinement of the structure in this space group left many parameters highly correlated. Thus, the $P1$ solution was transformed into the original $P\bar{1}$ cell by placing the midpoint between the two Zn positions at (0.5, 0.5, 0.5); refinement of the structure now proceeded smoothly.

All non-hydrogen atoms were refined anisotropically. Since not all the hydrogen atoms could be found from difference Fourier maps, their positions were calculated using idealized geometries based on packing considerations and d(C–H) = 0.95 Å. The positions were fixed for the final cycles of refinement. A final difference map was featureless. Fractional coordinates and isotropic thermal parameters for the non-hydrogen atoms are listed in Table 2; selected bond distances and angles are given in Table 3.

Table 2
Atomic fractional coordinates and isotropic thermal parameters for the non-hydrogen atoms in $[(C_3H_7)_4C_5H]_2Zn$

Atom	x	y	z	B_{eq} (Å^2)
Zn(1)	0.5458(1)	0.55268(9)	0.5135(1)	5.08(4)
C(1)	0.5011(3)	0.6345(3)	0.3425(4)	4.0(1)
C(2)	0.3716(3)	0.5839(3)	0.4127(4)	5.0(1)
C(3)	0.4163(3)	0.6852(3)	0.5841(3)	3.68(9)
C(4)	0.5665(3)	0.7896(3)	0.6121(3)	3.50(8)
C(5)	0.6198(3)	0.7567(3)	0.4621(3)	3.43(8)
C(6)	0.2034(3)	0.4943(3)	0.3035(4)	4.1(1)
C(7)	0.1911(4)	0.3839(4)	0.1439(5)	6.8(1)
C(8)	0.1306(5)	0.5773(4)	0.2542(5)	7.2(2)
C(9)	0.3093(3)	0.6750(3)	0.7000(4)	4.8(1)
C(10)	0.3768(5)	0.6673(4)	0.8621(5)	6.1(1)
C(11)	0.2537(4)	0.7856(4)	0.7349(5)	6.8(1)
C(12)	0.6499(4)	0.9223(3)	0.7680(4)	4.3(1)
C(13)	0.8115(4)	0.9519(3)	0.8644(4)	5.5(1)
C(14)	0.6578(5)	01.0436(3)	0.7237(5)	6.3(1)
C(15)	0.7748(3)	0.361(3)	0.4318(4)	4.0(1)
C(16)	0.8792(4)	0.7656(4)	0.4272(7)	7.4(2)
C(17)	0.7503(4)	0.8645(4)	0.2739(5)	6.7(1)

$B_{eq} = 8\pi^2/3\Sigma_{i=1}^{3}\Sigma_{j=1}^{3}U_{ij}a_i^* a_j^* \boldsymbol{a}_i \cdot \boldsymbol{a}_j$.

Table 3
Selected bond distances (Å) and angles (°) for $(Cp^{4i})_2Zn$

Atoms	Distance/angle
Zn(1)···Zn(1)′	1.115(2)
Zn(1)–C(1)	2.055(3)
Zn(1)···C(1)′	2.713(3)
Zn(1)–C(2)	1.991(4)
Zn(1)–C(2)′	2.223(4)
Zn(1)–C(3)	2.307(3)
Zn(1)···C(3)′	2.789(3)
Zn(1)···C(4)	2.514(3)
Zn(1)–C(5)	2.369(3)
Zn(1)–ring centroid	1.902
Zn(1)′–ring centroid	2.673
C(1)–C(2)	1.441(4)
C(1)–C(5)	1.386(4)
C(2)–C(3)	1.458(4)
C(3)–C(4)	1.402(4)
C(4)–C(5)	1.442(4)
C(ring)–CH (av.)	1.516(8)
CH–CH_3 (av.)	1.514(9)
C(1)–C(2)–C(3)	105.9(2)
C(2)–C(3)–C(4)	107.8(2)
C(3)–C(4)–C(5)	108.8(2)
C(4)–C(5)–C(1)	107.6(2)
C(5)–C(1)–C(2)	109.8(2)
CH_3–CH–CH_3 (av.)	110.5(9)
Planarity of rings	within 0.009 Å
Angle between ring plane and C(2)–Zn(1)′ bond	96.0°
Displacement of C(6) from ring plane	0.60 Å
Av. displacement of remaining methine carbons from ring plane	0.06 Å

3. Results

3.1. Synthesis of $(Cp^{3i})_2Zn$ and $(Cp^{4i})_2Zn$

The high-yield synthesis of the isopropylated zinc metallocenes $(Cp^{3i})_2Zn$ and $(Cp^{4i})_2Zn$ was readily ac-

complished by the metathetical reaction of either KCp^{3i} or KCp^{4i} with ZnI_2 in Et_2O (Eq. (1)):

$$2\,KCp^{ni} + ZnI_2 \xrightarrow[n=3,4]{Et_2O} (Cp^{ni})_2Zn + 2\,KI\downarrow \qquad (1)$$

The metallocenes were isolated by hexanes extraction of the reaction mixtures. Purification of $(Cp^{4i})_2Zn$ was carried out by fractional sublimation (100–140°C, 10^{-6} Torr) or by recrystallization from THF, yielding the metallocene as an ivory–white, crystalline solid (m.p. 123–125°C). In contrast, $(Cp^{3i})_2Zn$ was isolated from hexanes as a pale yellow oil; although the complex could be purified by high vacuum distillation (100°C, 10^{-6} Torr), such distillations invariably resulted in considerable mechanical losses of product. Fortunately, $(Cp^{3i})_2Zn$ was usually obtained directly from the hexanes extract in sufficient purity (above 98%) to render further purification unnecessary. Like $(Cp^{3i})_2Ca$ [19], samples of $(Cp^{3i})_2Zn$ allowed to stand for extended periods (1–2 months) at ambient temperature partially solidified, forming opaque chunks of wax-like solid (m.p. ca. 30°C). Analytical and spectroscopic data (^1H and ^{13}C NMR, IR) for $(Cp^{3i})_2Zn$ and $(Cp^{4i})_2Zn$ confirmed the proposed formulations.

$(Cp^{3i})_2Zn$ and $(Cp^{4i})_2Zn$, like their Group 2 and Group 14 counterparts [15,16], exhibit dramatically different physical characteristics stemming from the inherent differences in conformational flexibility for the $[Cp^{3i}]^-$ and $[Cp^{4i}]^-$ ligands. However, essentially no difference in air-stability is found for the two zinc metallocenes, as both begin to decompose almost instantaneously on exposure to the atmosphere. This result suggests that encapsulation of the metal in $(Cp^{4i})_2Zn$ by the two $[Cp^{4i}]^-$ ligands is not occurring to the extent found for the analogous Group 2 and Group 14 metallocenes, most likely a consequence of a "slipped-sandwich" geometry [13,14]. This supposition was confirmed by single crystal X-ray structural determination of $(Cp^{4i})_2Zn$ (see below).

3.2. Variable-temperature NMR study of the solution behavior of $(Cp^{4i})_2Zn$

In spite of the presumably asymmetric bonding of the cyclopentadienyl ligands in $(Cp^{3i})_2Zn$ and $(Cp^{4i})_2Zn$, only one set of resonances for the $[Cp^{3i}]^-$ and $[Cp^{4i}]^-$ ligands is found in the NMR spectra of the complexes at room temperature. Thus, the metallocenes must be undergoing one or more fluxional processes that equilibrate the Cp' ligands and are fast on the NMR timescale. Recent molecular dynamics calculations on the related slipped-sandwich complex Cp_2Be identified two such possible mechanisms: a gear-wheel shift, in which the bond between the metal and the η^1-ring migrates from one carbon to the next, and a molecular inversion process, which interchanges the η^1- and η^5-rings through an η^3,η^3-transition state [20]. The activation barriers for these processes were calculated to be 5 and 8 kJ mol^{-1} respectively. Consistent with such low energetic barriers, variable-temperature NMR studies of beryllocene [21] and several zinc metallocenes [13,14] could not stop the fluxional behavior of the complexes in solution.

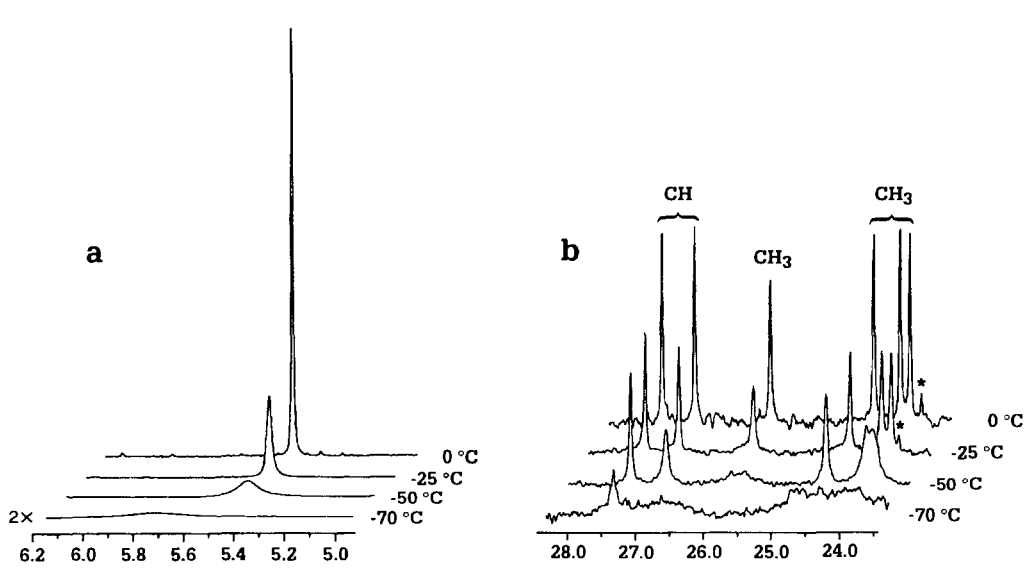

Fig. 2. Variable-temperature NMR spectra of $(Cp^{4i})_2Zn$ in toluene-d_8: (a) ^1H NMR spectra of the cyclopentadienyl proton resonance; (b) ^{13}C NMR spectra of the methyl and methine carbon resonances. The starred peak is an impurity in the solvent.

We were curious whether the presence of the extremely bulky $[Cp^{4i}]^-$ ligands in $(Cp^{4i})_2Zn$ could increase the activation energy of the fluxional processes to the point where they would become detectable by NMR spectroscopy. Therefore, a variable-temperature NMR study of $(Cp^{4i})_2Zn$ in toluene-d_8 was conducted. All the resonances in the ^1H NMR spectrum of $(Cp^{4i})_2Zn$ broaden as the temperature is lowered below 0°C; this broadening is most severe for the ring hydrogen resonance, which is almost indistinguishable from the baseline at −70°C (Fig. 2). This resonance also shifts downfield as the temperature is lowered, from a value of 5.45 ppm at 25°C to 5.77 ppm at −70°C. However, no explicit decoalesence of any of the ^1H NMR resonances is observed over the +25 to −70°C temperature range studied here.

Similar results were obtained for the ^{13}C NMR spectra of $(Cp^{4i})_2Zn$ over the same temperature range; although the peaks broaden as the temperature is decreased, no definitive decoalesence is observed down to −70°C. Interestingly, the collapse of the methine and methyl carbon resonances in the spectra is not symmetrical (Fig. 2). The more upfield of the two CH peaks (at 27.3 ppm) broadens more rapidly than the downfield CH resonance, disappearing into the baseline below −50°C. Additionally, the most downfield of the four CH_3 peaks (at 26.2 ppm) collapses much faster than the remaining three CH_3 peaks; this resonance is already broadened at 0°C and becomes unobservable below −25°C. It is possible that this peak decoalesces into two resonances at −50°C, as an extremely broad feature resembling two weak intensity resonances is found at approximately 26 ppm in the spectrum (Fig. 2). However, these peaks are not observed at −70°C, which makes their identification tentative.

3.3. Structure of $(Cp^{4i})_2Zn$

An X-ray crystal structure determination of $(Cp^{4i})_2Zn$ revealed that this complex has a "slipped-sandwich" geometry, with η^1- and approximately η^5-coordinated cyclopentadienyl rings (Fig. 3). The molecule has a crystallographically imposed center of inversion, which equates the two coplanar $[Cp^{4i}]^-$ ligands. The zinc atom is disordered across the inversion center at positions that exchange the coordination modes of the two cyclopentadienyl rings. This means that the observed geometry of the $[Cp^{4i}]^-$ ligand is a composite of the individual geometries present in the centrally bonded (η^5) and peripherally bonded (η^1) rings. The same type of disorder also occurs in the slipped-sandwich structures of $(Me_4PhC_5)_2Zn$ [14] and Cp_2Be [8]. A summary of the bond distances and angles for $(Cp^{4i})_2Zn$ is given in Table 3.

The Zn–C(2)′ bond distance of 2.223(4) Å is the sole bonding interaction for the η^1-ring in $(Cp^{4i})_2Zn$; the

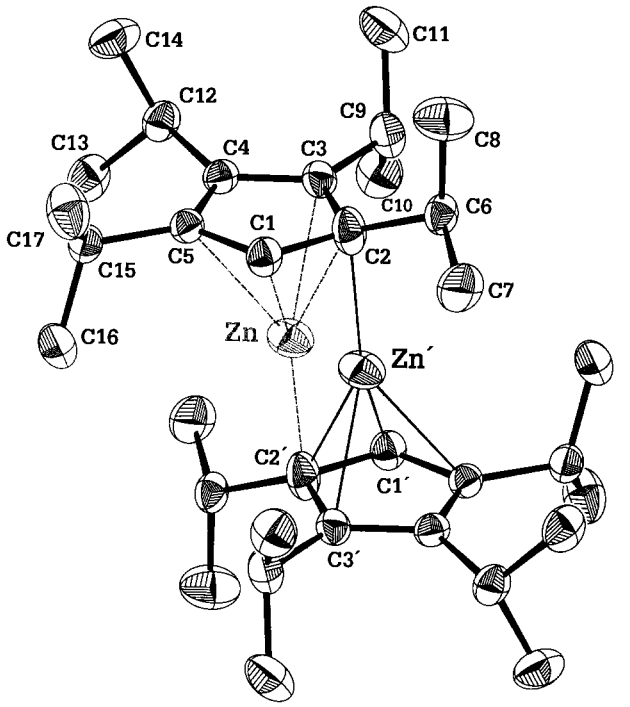

Fig. 3. ORTEP diagram of the non-hydrogen atoms of $(Cp^{4i})_2Zn$, giving the numbering scheme used in the text. Thermal ellipsoids are shown at the 35% level; one site for the disordered zinc atom is shaded gray.

remaining Zn–C distances for this ring are greater than 2.7 Å and are non-bonding. This Zn–C distance is appreciably longer than the analogous Zn–C distance of 2.094(3) Å found for the η^1-bonded cyclopentadienyl ligand in $(Me_4PhC_5)_2Zn$ [14]. Similarly short Zn–C distances have been found for the monohapto rings in the gas phase structures of Cp^*_2Zn (2.04(6) Å) and $[(Me_3Si)C_5H_4]_2Zn$ (2.07(10) Å) [13]. The lengthening of the Zn–C interaction in $(Cp^{4i})_2Zn$ apparently occurs to relieve the steric pressure caused by the increased bulk of the $[Cp^{4i}]^-$ ligand. As a result, the peripherally bonded $[Cp^{4i}]^-$ ligand is only weakly bound to the zinc atom.

The interaction of the zinc with the more centrally bound ring in $(Cp^{4i})_2Zn$ is also noteworthy, in that the zinc is shifted from pentahapto coordination towards one edge (C(1)–C(2)) of the $[Cp^{4i}]^-$ ligand. This leads to a wide range of observed Zn–C distances for this ring, from 1.991(4) Å for Zn–C(2) to 2.514(3) Å for Zn–C(4); the latter distance is long enough to be considered non-bonding [22–24]. In contrast, the corresponding range of Zn–C distances for the η^5-ring in $(Me_4PhC_5)_2Zn$ is much narrower (2.093(3) to 2.299(3) Å). It should be noted that the Zn–C(2) bond distance of 1.991(4) Å in $(Cp^{4i})_2Zn$ is the shortest Zn–C ring bond yet reported for a cyclopentadienyl zinc complex, and is only 0.06 Å longer than the 1.930(2) Å distance found for the Zn–C σ-bond in dimethylzinc [25].

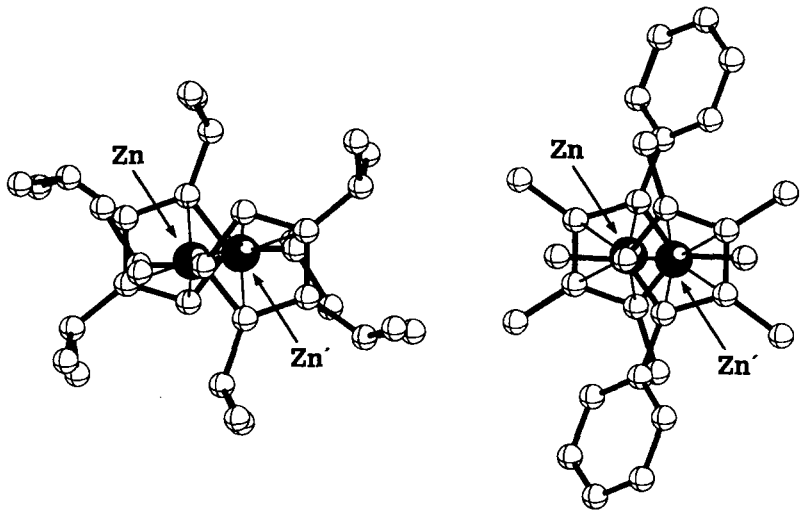

Fig. 4. Ball-and-stick projections of $(Cp^{4i})_2Zn$ (left) and $(Me_4PhC_5)_2Zn$ (right) illustrating the greater degree of "ring-slippage" in the former.

Interpretation of the metrical parameters of the $[Cp^{4i}]^-$ ligand of $(Cp^{4i})_2Zn$ is affected by the fact that the observed structure represents a superposition of the centrally bonded and peripherally bonded rings. Nevertheless, the C–C bond distances are clearly not equal; the C(1)–C(5) (1.386(4) Å) and C(3)–C(4) (1.402(4) Å) bonds are shorter than those observed for C(1)–C(2) (1.441(4) Å), C(2)–C(3) (1.458(4) Å), and C(4)–C(5) (1.442(4) Å). Similar but less pronounced bond alternation was also detected for the ring carbon–carbon bonds in $(Me_4PhC_5)_2Zn$ and Cp_2Be. The alternating pattern of ring C–C distances is consistent with a partial localization of the charge of the cyclopentadienyl ring onto C(2), which forms the closest bond to the zinc atom in both $[Cp^{4i}]^-$ ligands. However, the C–C bond alteration in $(Cp^{4i})_2Zn$ is still significantly less than that found in cyclopentadiene itself, which has single and double C–C bond lengths of 1.51 and 1.34 Å respectively [26]. Also consistent with the structural data is the lack of bands in the 1500–1600 cm^{-1} region of the IR spectrum of $(Cp^{4i})_2Zn$, which indicates the absence of localized C=C double bonds.

The orientation angles [27] of the isopropyl groups on C(3), C(4) and C(5) are nearly perpendicular to the ring plane (angles of 88.4°, 89.1° and 82.1° respectively). In contrast, the orientation angle for the C(6)–C(7)–C(8) isopropyl group bound to C(2) is only 68.4°; this isopropyl group is also dislocated from the plane of the ligand, as evidenced by the 0.60 Å displacement of the C(6) methine carbon above the ring (equivalent to a 23° bend). The resulting distorted tetrahedral geometry around C(2) is consistent with some partial sp^3 hybridization for this atom. However, the long Zn–C(2)′ bond distance, and the small angle this bond makes with the plane of the ring (96.0°), suggest that any sp^3 hybridization of the C(2) carbon in limited. In addition, and probably more importantly, the bending of the C(6)–C(7)–C(8) isopropyl group relieves the steric congestion caused by its position directly above the other cyclopentadienyl ring.

4. Discussion

4.1. Comparative physical properties of $(Cp^{3i})_2Zn$ and $(Cp^{4i})_2Zn$

The intriguing differences in physical characteristics observed for the alkaline-earth metallocenes $(Cp^{4i})_2M$ and $(Cp^{3i})_2M$ are duplicated in the zinc analogs described here. Interestingly, $(Cp^{3i})_2Zn$ has a lower melting point (ca. 30°C) than $(Cp^{3i})_2Mg$ (92–100°C) [19], in spite of the similar size of the metals. This suggests that the conformational flexibility of the $[Cp^{3i}]^-$ ligands is greater in the presumably "slipped-sandwich" geometry of $(Cp^{3i})_2Zn$ than it is in $(Cp^{3i})_2Mg$, where both rings are probably η^5-coordinated to the metal. The high air-sensitivity exhibited by both $(Cp^{3i})_2Zn$ and $(Cp^{4i})_2Zn$, however, is an instance where a conspicuous difference between the $(Cp^{4i})_2M$ and $(Cp^{3i})_2M$ metallocenes is not reproduced for zinc. The increased air-sensitivity of $(Cp^{4i})_2Zn$ is evidently also caused by the slipped geometry of the complex, which prevents the $[Cp^{4i}]^-$ ligand from effectively encapsulating the metal center.

4.2. The effect of the bulky $[Cp^{4i}]^-$ ligands on the structure of $(Cp^{4i})_2Zn$

The increased steric pressure of the $[Cp^{4i}]^-$ ligands in $(Cp^{4i})_2Zn$ causes some notable differences in its

"slipped-sandwich" structure when compared with those found previously for Cp_2Be and $(Me_4PhC_5)_2Zn$. These differences are the result of an increased slippage of the cyclopentadienyl rings in $(Cp^{4i})_2Zn$, where "ring-slippage" is defined as the distance between the ring centroid and the perpendicular projection of the metal atom on the least-squares plane of the ring [14]. The ring-slippage is 1.50 Å for the η^1-ring and 0.52 Å for the approximately η^5-ring of $(Cp^{4i})_2Zn$; both values are ca. 0.30 Å larger than the corresponding distances of 1.21 and 0.20 Å for $(Me_4PhC_5)_2Zn$ [14]. The structural differences between $(Cp^{4i})_2Zn$ and $(Me_4PhC_5)_2Zn$ caused by the variation in ring-slippage are particularly evident on examination of the two complexes perpendicular to the plane of the Cp rings, as illustrated in Fig. 4.

The increased lateral separation of the $[Cp^{4i}]^-$ ligands in $(Cp^{4i})_2Zn$ is apparently necessary to avoid undue steric crowding in the complex. Most noticeably, the increased ring-slippage reduces the interaction of the C(9)–C(10)–C(11) isopropyl group with the ring carbons of the other $[Cp^{4i}]^-$ ligand. The increased ring-slippage in $(Cp^{4i})_2Zn$ also increases the separation between the C(6)–C(7)–C(8) isopropyl group and the isopropyl groups bound to the C(4) and C(5) ring carbons of the second $[Cp^{4i}]^-$ ligand. The fact that the structure of $(Cp^{4i})_2Zn$ can be distorted to the extent necessary to prevent these unfavorable interactions suggests that the bonding between the zinc atom and the $[Cp^{4i}]^-$ ligands in the complex is still predominately ionic.

The increased ring-slippage in $(Cp^{4i})_2Zn$ results in some unexpected distances for the zinc–carbon ring bonds, especially when compared with $(Me_4PhC_5)_2Zn$. Most notable is the fact that two of the Zn–C bonds for the more centrally bound $[Cp^{4i}]^-$ ligand (Zn–C(2), 1.991(4) Å and Zn–C(1), 2.055(3) Å) are shorter than the Zn–C bond of the peripherally bonded ligand (Zn–C(2)′, 2.223(4) Å). For Cp_2Be and $(Me_4PhC_5)_2Zn$, partial covalency in the metal–cyclopentadienyl interactions has been assumed to be present only for the η^1-ring;, i.e. the M–Cp bonding for the η^5-ring is regarded as almost completely ionic. This assumption is not as obviously valid for $(Cp^{4i})_2Zn$, however, as the Zn–C bond distances suggest that the η^5-ring, and not the η^1-ring, has the more covalent interaction with the metal. Thus, the structure of $(Cp^{4i})_2Zn$ raises the possibility that the covalent contribution to the bonding in slipped-sandwich metallocenes does not have to be restricted to only one cyclopentadienyl ligand.

The length of the Zn–C(2)′ bond in $(Cp^{4i})_2Zn$ also suggests that even a small amount of increased ring-slippage of the cyclopentadienyl ligands could lead to loss of the polyhapto coordination of the $[Cp^{4i}]^-$ ring to the zinc atom. Thus, attempts to synthesize zinc metallocenes with Cp ligands that are bulkier than $[Cp^{4i}]^-$ may be prohibited due to "steric oversaturation", i.e. the bulk of the intended ligands will be greater than can be accommodated around the metal center [28]. A similar argument for beryllium has been used to rationalize the inability to synthesize decamethylberyllocene Cp^*_2Be by routes that are successful with larger metals [29].

The substantial bulk of the $[Cp^{4i}]^-$ ligands in $(Cp^{4i})_2Zn$ should also decrease the rate of the fluxional processes that equilibrate the Cp′ rings in solution, at least when compared with slipped-sandwich complexes with less bulky rings. This is because the transition state structures for both fluxional processes (e.g. η^2,η^5-coordination for the gear-wheel shift; η^3,η^3-coordination for molecular inversion) involve a decrease in the lateral separation of the cyclopentadienyl rings from the ground state structure [20]. Considering the increased ring-slippage in the solid state structure of $(Cp^{4i})_2Zn$, it follows that decreasing the lateral separation of the $[Cp^{4i}]^-$ ligands in this complex should be more energetically unfavorable than in less-encumbered complexes, leading to higher activation barriers for the fluxional processes.

Unfortunately, attempts to verify this effect experimentally by variable temperature NMR experiments on $(Cp^{4i})_2Zn$ were not completely successful. On cooling below 0°C, a gradual broadening of the proton NMR resonances of $(Cp^{4i})_2Zn$ occurs; below −50°C this broadening becomes much more severe. This behavior is consistent with what might be the onset of decoalescence in the spectra from the freezing out of a dynamic process in solution, although some solubility loss of the compound may contribute to the broadening. The apparent temperature for this process (ca. −50 to −70°C) is similar to that previously observed in variable temperature ^1H NMR experiments on $(Cp^{4i})_2Ca$ and $(Cp^{4i})_2Ba$ [15]. For these complexes, the changes in the NMR spectra were assigned to the appearance of hindered rotation of the $[Cp^{4i}]^-$ isopropyl groups around the ring–$CH(Me)_2$ bonds; the experimentally determined activation barriers were ca. 46 kJ mol^{-1} for both complexes. It is reasonable to assume that the observed changes in the proton NMR spectra of $(Cp^{4i})_2Zn$ are also caused by hindered rotation of the isopropyl groups, and not by freezing out of the fluxional processes that are equilibrating the rings.

In contrast to the behavior observed in the ^1H NMR spectra, the rate of broadening was not constant for the methine and methyl carbon resonances in the ^{13}C NMR spectra of $(Cp^{4i})_2Zn$ at lower temperatures; one CH and CH_3 peak collapse more rapidly than the remaining methine and methyl resonances (Fig. 2). This behavior suggests that on average one $[Cp^{4i}]^-$ isopropyl group of $(Cp^{4i})_2Zn$ has a higher activation energy for rotation around the ring–$CH(Me)_2$ bond than the remaining substituents. In the solid state structure of $(Cp^{4i})_2Zn$,

one isopropyl substituent of the $[Cp^{4i}]^-$ ligands, specifically the C(6)–C(7)–C(8) isopropyl group opposite the other $[Cp^{4i}]^-$ ring, is notably more sterically crowded than the other substituents; rotation of this group is likely to be energetically more unfavorable than analogous rotations for the remaining ring substituents. The observed variable temperature behavior of $(Cp^{4i})_2Zn$ is therefore consistent with an average geometry for $(Cp^{4i})_2Zn$ in solution, that is analogous to the asymmetric "slipped-sandwich" geometry observed in the solid state.

5. Conclusions

Zincocenes containing the bulky $[Cp^{3i}]^-$ and $[Cp^{4i}]^-$ ligands extend the types of metallocene whose physical properties and structures can be directly influenced by steric forces. The "slipped-sandwich" structure of $(Cp^{4i})_2Zn$ does not confer the same degree of protection on the metal center observed with the corresponding Group 2 or Group 14 metallocenes. The comparatively long η^1- and short η^5-bond distances in $(Cp^{4i})_2Zn$ suggest that describing the Zn–Cp ring interaction for each ring solely in "ionic" or "covalent" terms is not realistic, and that both electronic and steric effects must be considered when interpreting the bonding in metallocenes of electropositive metals.

Acknowledgments

D.J.B. is the grateful recipient of an NSF Predoctoral Fellowship. Funds for the X-ray diffraction facility at Vanderbilt University were provided through NSF Grant CHE-8908065. We thank Dr. Markus Voehler for assistance with the NMR experiments.

References and note

[1] E.O. Fischer and H.P. Hofmann, *Chem. Ber., 92* (1959) 482.
[2] A. Almenningen, O. Bastiansen and A. Haaland, *J. Chem. Phys., 40* (1964) 3434.
[3] A. Haaland, *Acta Chem. Scand., 22* (1968) 3030.
[4] D.S. Marynick, *J. Am. Chem. Soc., 99* (1977) 1436.
[5] N.-S. Chiu and H.F. Schaefer, III, *J. Am. Chem. Soc., 100* (1978) 2604.
[6] E.D. Jemmis, S. Alexandratos, P.v.R. Schleyer, A. Streitwieser, Jr. and H.F. Schaefer, III, *J. Am. Chem. Soc., 100* (1978) 5695.
[7] R. Gleiter, M.C. Böhm, A. Haaland, R. Johansen and J. Lusztyk, *J. Organomet. Chem., 170* (1979) 285.
[8] K.W. Nugent, J.K. Beattie, T.W. Hambley and M.R. Snow, *Aust. J. Chem., 37* (1984) 1601.
[9] J. Lustyk and K.B. Starowieyski, *J. Organomet. Chem., 170* (1979) 293.
[10] K.W. Nugent and J.K. Beattie, *Inorg. Chem., 27* (1988) 4269.
[11] J.K. Beattie and K.W. Nugent, *Inorg. Chim. Acta, 198–200* (1992) 309.
[12] R. Blom, A. Haaland and J. Weidlein, *J. Chem. Soc., Chem. Commun.*, (1985) 266.
[13] R. Blom, J. Boersma, P.H.M. Budzelaar, B. Fischer, A. Haaland, H.V. Volden and J. Weidlein, *Acta Chem. Scand., A40* (1986) 113.
[14] B. Fischer, P. Wijkens, J. Boersma, G. van Koten, W.J.J. Smeets, A.L. Spek and P.H.M. Budzelaar, *J. Organomet. Chem., 376* (1989) 223.
[15] R.A. Williams, K.F. Tesh and T.P. Hanusa, *J. Am. Chem. Soc., 113* (1991) 4843.
[16] D.J. Burkey and T.P. Hanusa, *Organometallics, 14* (1995) 11.
[17] D.J. Burkey and T.P. Hanusa, *Comments Inorg. Chem., 17* (1995) 41.
[18] J. Sandström, *Dynamic NMR Spectroscopy*, Academic Press, London, 1982.
[19] D.J. Burkey, T.P. Hanusa and J.C. Huffman, *Adv. Mater. Opt. Electron., 4* (1994) 1.
[20] P. Margl, K. Schwarz and P.E. Blöchl, *J. Am. Chem. Soc., 116* (1994) 11177.
[21] C. Wong and S. Wang, *Inorg. Nucl. Chem. Lett., 11* (1975) 677.
[22] P.H.M. Budzelaar, J. Boersma, G.J.M. van der Kerk, A.L. Spek and A.J.M. Duisenberg, *J. Organomet. Chem., 281* (1985) 123.
[23] P.H.M. Budzelaar, J. Boersma, G.J.M. van der Kerk and A.L. Spek, *Organometallics, 3* (1984) 1187.
[24] Based on distance criteria, the bonding to the ring could be designated as "η^4". Because of the borderline nature of the case, however, the polyhapto ring will be referred to throughout the text as bound "η^5".
[25] A. Almenningen, T.U. Helgaker, A. Haaland and S. Samdal, *Acta Chem. Scand., A36* (1982) 159.
[26] D. Damiani, L. Feretti and E. Gallinella, *Chem. Phys. Lett., 37* (1976) 265.
[27] D.J. Burkey, R.A. Williams and T.P. Hanusa, *Organometallics, 12* (1993) 1331.
[28] T.P. Hanusa, *Chem. Rev., 93* (1993) 1023.
[29] C.J. Burns and R.A. Andersen, *J. Organomet. Chem., 325* (1987) 31.